Title

Simultaneous phase-contrast MRI and PET for noninvasive quantification of cerebral blood flow and reactivity in healthy subjects and patients with cerebrovascular disease

Journal

Journal of Magnetic Resonance Imaging, 51(1)

ISSN

1053-1807

Authors

Ishii, Yosuke
Thamm, Thoralf
Guo, Jia
et al.

Publication Date

2020

DOI

10.1002/jmri.26773

Peer reviewed

HHS Public Access

Author manuscript

J Magn Reson Imaging. Author manuscript; available in PMC 2020 May 11.

Published in final edited form as:

J Magn Reson Imaging. 2020 January ; 51(1): 183–194. doi:10.1002/jmri.26773.

Simultaneous Phase-Contrast MRI and PET for Noninvasive Quantification of Cerebral Blood Flow and Reactivity in Healthy Subjects and Patients With Cerebrovascular Disease

Yosuke Ishii, MD, PhD[1,2,*], **Thoralf Thamm**[1,3], **Jia Guo, PhD**[1,4], **Mohammad Mehdi Khalighi, PhD**, **Mirwais Wardak, PhD**[5,1], **Dawn Holley, BS, CNMT**[1], **Harsh Gandhi, MS**[1], **Jun Hyung Park, PhD**[1], **Bin Shen, PhD**[1], **Gary K. Steinberg, MD, PhD**[6], **Frederick T. Chin, PhD**[1], **Greg Zaharchuk, MD, PhD**[1], **Audrey Peiwen Fan, PhD**[1]

[1]Department of Radiology, Stanford University, Stanford, California, USA

[2]Department of Neurosurgery, Tokyo Medical and Dental University, Tokyo, Japan

[3]Center for Stroke Research Berlin (CSB), Charité - Universitätsmedizin Berlin, Berlin, Germany

[4]Department of Bioengineering, University of California Riverside, Riverside, California, USA

[5]Global Applied Science Lab, GE Healthcare, Menlo Park, California, USA

[6]Department of Neurosurgery, Stanford University, Stanford, California, USA

Abstract

Background: $H_2{}^{15}O$-positron emission tomography (PET) is considered the reference standard for absolute cerebral blood flow (CBF). However, this technique requires an arterial input function measured through continuous sampling of arterial blood, which is invasive and has limitations with tracer delay and dispersion.

Purpose: To demonstrate a new noninvasive method to quantify absolute CBF with a PET/MRI hybrid scanner. This blood-free approach, called PC-PET, takes the spatial CBF distribution from a static $H_2{}^{15}O$-PET scan, and scales it to the whole-brain average CBF value measured by simultaneous phase-contrast MRI.

Study Type: Observational.

Subjects: Twelve healthy controls (HC) and 13 patients with Moyamoya disease (MM) as a model of chronic ischemic disease.

Field Strength/Sequences: 3T/2D cardiac-gated phase-contrast MRI and $H_2{}^{15}O$-PET.

Assessment: PC-PET CBF values from whole brain (WB), gray matter (GM), and white matter (WM) in HCs were compared with literature values since 2000. CBF and cerebrovascular reactivity (CVR), which is defined as the percent CBF change between baseline and post-

[*]Address reprint requests to: Y.I., Department of Radiology, Stanford University, 1201 Welch Rd., Stanford, CA 94305-5488. yishii0712@gmail.com.

Declaration of Conflicting Interests

The author(s) declared the following potential conflicts of interest with respect to the research, authorship, and/or publication of this article: Mohammad Mehdi Khalighi is employed by GE Healthcare. Greg Zaharchuk received funding support from GE Healthcare.

acetazolamide (vasodilator) scans, were measured by PC-PET in MM patients and HCs within cortical regions corresponding to major vascular territories.

Statistical Tests: Linear, mixed effects models were created to compare CBF and CVR, respectively, between patients and controls, and between different degrees of stenosis.

Results: The mean CBF values in WB, GM, and WM in HC were 42 ± 7 ml/100 g/min, 50 ± 7 ml/100 g/min, and 23 ± 3 ml/100 g/min, respectively, which agree well with literature values. Compared with normal regions (57 ± 23%), patients showed signi$_{fi}$cantly decreased CVR in areas with mild/moderate stenosis (47 ± 17%, $P = 0.011$) $_{\text{and in}}$ severe/occluded areas (40 ± 16, $P = 0.016$).

Data Conclusion: PC-PET identifies differences in cerebrovascular reactivity between healthy controls and cerebrovascular patients. PC-PET is suitable for CBF measurement when arterial blood sampling is not accessible, and warrants comparison to fully quantitative $H_2{}^{15}O$-PET in future studies.

Level of Evidence: 3

Technical Efficacy Stage: 2

CEREBRAL BLOOD FLOW (CBF) is a critical factor to evaluate the severity of ischemia and manage the treatment of patients with cerebrovascular disease.[1] Moyamoya (MM) disease is a progressive occlusive cerebrovascular arteriopathy, characterized by stenosis of distal internal carotid and proximal cerebral arteries and compensatory dilation of collateral vessels termed MM vessels.[2] In chronic ischemic cerebrovascular diseases like MM, vasodilation creates a decrease in cerebral perfusion pressure, while CBF is maintained.[1] In these pathological conditions, further vasodilation is limited, such that decreased cerebrovascular reactivity (CVR) is a sensitive indicator of disease progression. CVR is thus useful to predict the risk of future infarction and to manage surgical intervention.[3]

Autoradiography with O-15 water positron emission tomography ($H_2{}^{15}O$-PET) is an established method to measure the absolute value of CBF.[4] Traditionally, CBF quantification with $H_2{}^{15}O$-PET requires an arterial input function (AIF), typically measured through the continuous sampling of arterial blood. Arterial sampling is invasive and is not always possible. In addition, it has inherent limitations, with the delay and dispersion of the tracer as it travels to the brain because arterial blood is typically sampled from the radial artery at the wrist.[5] Although several quantitative $H_2{}^{15}O$-PET methods without arterial blood sampling such as population-based input functions have been designed, these approaches have the drawback of ignoring individual AIF variation.[6] Image-derived input function (IDIF) methods that identify brain feeding arteries in the PET field of view by time-of-flight (TOF) magnetic resonance imaging (MRI) have also been proposed. While promising, the IDIF approaches are sensitive to registration errors and artifacts due to spill-in and spill-out effects with limited spatial resolution. Consequently, the use of IDIF for CBF measurements is not widely adopted and relatively few studies have achieved successful results in clinical practice using simultaneous PET-MRI acquisition.[7]

Instead of blood sampling, simultaneous PET-MRI offers an alternative method to achieve absolute quantification of CBF. Phase-contrast MRI (PC-MRI) can measure blood flow

velocity and vessel area quickly and noninvasively. The reliability and reproducibility of blood inflow obtained from PC-MRI has been established by various validation studies.[8,9] PC-MRI has been used to measure global CBF by normalizing the total blood inflow of bilateral internal carotid arteries (ICAs) and vertebral arteries (VAs) to whole-brain (WB) weight.[10,11] Total brain blood flow from PC-MRI has been used to estimate labeling efficiency and scale global CBF measurements by arterial spin labeling MRI,[12,13] including on simultaneous PETMRI platforms.[14] More recently, Ssali et al combined PC-MRI with simultaneous observations of regional CBF distribution (ie, with a concurrent $H_2{}^{15}O$-PET scan) to create quantitative perfusion maps on a PET-MRI scanner.[11] Ssali et al reported good agreement between PC-MRI scaling and the PET reference using arterial blood sampling in animal models. However, the method remains to be demonstrated in human subjects and cerebrovascular patients, for which PC-MRI has shown value to understand abnormal total blood inflow.[15]

In this study we measured absolute CBF and CVR in healthy volunteers and patients with MM disease using a blood-free, noninvasive PET/MRI approach. With this technique, each static $H_2{}^{15}O$-PET scan is scaled using global CBF measured by simultaneously acquired PC-MRI. We hypothesized 1) that this new method gives absolute CBF values in the physiologically expected range for normal controls, with expected variation with age and hematocrit, and 2) that it is sensitive to regional cerebral blood flow disturbance in cerebrovascular disease.

Materials and Methods

Subjects

This study was performed in compliance with the Stanford University Institutional Review Board. All subjects provided written informed consent before the imaging examination. Data were acquired from 12 healthy controls (HCs) and 13 preoperative patients with MM disease. Patients were recruited through the Stanford Neuroscience clinics. The characteristics of the study population are shown in Table 1. There were no statistical differences in demographics between the two groups. The diagnosis of MM disease was based on one or more of following imaging modalities: cerebral angiogram, MR angiogram, and computed tomography angiogram. Inclusion criteria included age of 15 years and ability to comply with all studies. Exclusion criteria included known allergies to sulfa drugs or contrast agents, previous brain surgery, impaired renal function that would preclude administration of contrast agent, or any contraindication to MRI. Participants were requested to refrain from caffeine intake for 6 hours before the study and a venous blood sample (2–3 ml) was taken to measure the subject’s hematocrit.

PET Acquisition

All PET and MR images were acquired on a simultaneous TOF enabled 3.0T PET/MRI system (Signa, GE Healthcare, Waukesha, WI). Two CBF studies were performed on each subject: one baseline scan and one scan 20 minutes after intravenous administration of acetazolamide (ACZ, 15 mg/kg), a vasodilator. Each subject received an intravenous injection of $H_2{}^{15}O$ (863 ± 112 MBq) with a bolus duration of 30 seconds for each PET

acquisition through the antecubital vein. PET acquisition commenced with the tracer injection, and static PET images were reconstructed from 2 minutes of detected counts after the $H_2{}^{15}O$ injection with the following parameters: matrix size: 192 × 192, field-of view (FOV): 300 mm, and slice thickness: 2.78 mm. PET reconstruction was performed with a TOF-ordered subset expectation maximization (TOF-OSEM) algorithm (four iterations, 28 subsets) and included corrections for decay, scatter, random counts, dead time, and point spread function compensation. During each PET scan, a 2-point Dixon MRI scan was acquired for attenuation correction using an atlas-based algorithm.[16]

MRI Acquisition

PC-MRI was used for quantitative assessment of flow velocity in the ICAs and VAs. Two PC-MRI scans were acquired in each patient, concurrent with the baseline and post-ACZ injection $H_2{}^{15}O$-PET scans. Cardiac-gated fast low-angle gradient echo sequences with the following parameters were used: repetition time (TR) = 12 msec, echo time (TE) = 4.6 msec, flip angle = 20, matrix size = 480 × 384, voxel size = 0.375 × 0.375 × 3.0 mm, number of slices = 1, and number of averages = 2. Velocity encoding (Venc) was set at 100 cm/s in the inferior-to-superior direction. Ten single 2D velocity-encoded phase images were acquired per cardiac cycle for a total acquisition time of 90–150 seconds, depending on the subject's heart rate. The imaging slices were placed between the common carotid artery bifurcation and the flexion of VA at the second cervical vertebrae, perpendicular to the ICAs and VAs, as confirmed by cervical MR angiogram (MRA).

A T_1-weighted anatomical scan based on fast spoiled gradient-echo brain volume imaging was used for estimation of WB weight and as a brain mask. The imaging parameters were as follows: TR = 9.6 msec, TE = 3.8 msec, flip angle = 13, voxel size = 0.94 × 0.94 × 1 mm. TOF intracranial MR angiograms were also acquired for clinical evaluation of patients, with the following parameters: TR = 22 msec, TE = 2.4 msec, flip angle = 15, bandwidth = 195 Hz/pixel, and voxel size = 0.43 × 0.43 × 1.2 mm.

Data Processing

TOTAL BLOOD INFLOW AND BRAIN WEIGHT.

All PC-MRI flow data were analyzed with a web-based medical imaging analytics platform (Arterys, San Francisco, CA) using semiautomatically drawn regions of interest (ROIs) corresponding to the lumen of each vessel. The software provided measurements of the average bulk blood flow (ml/min) within the vessels, the blood flow velocity at each cardiac phase, and the cross-sectional area of the vessel lumen. We also measured maximum deviation angle manually from maximum-intensity-projection images of neck MRA relative to the image acquisition plane of phase-contrast MRI using OsiriX lite v. 10.0.3 software (Pixmeo, Geneva, Switzerland).

Total blood inflow was calculated as the sum of the bulk blood volume flow measurements in the bilateral ICAs and VAs. Total brain volume was measured using the total voxel count of the masked T_1-weighted structural image using FSL's Brain Extraction Toolbox (BET)

and Cluster software (FMRIB Software Library, Oxford, UK). Brain volume was used to calculate the total brain weight (g) assuming brain tissue density of 1.1 g/ml.

PC-PET.

The PC-PET method calculates absolute CBF maps using information from both PET and MRI. The 2-minute static $H_2{}^{15}O$-PET maps, reflecting relative CBF distribution, were scaled to have mean whole brain CBF (WB-CBF) consistent with PC-MRI measurements (Fig. 1).

First, total blood inflow from PC-MRI was divided by total brain weight to calculate WB-CBF (ml/100 g/min). Next, the WB-CBF was divided by the mean value of the 2-minute static PET counts across the WB, yielding a scan-specific scaling factor. This WB mask included the cerebellum and ventricles but excluded the skull and skin. Finally, the relative CBF map from the static $H_2{}^{15}O$-PET acquisition was multiplied by the scaling factor to create the quantitative CBF map (in units of ml/100 g/min). We called this method "PC-PET," where each PC-PET CBF map has the same mean WB CBF value as the corresponding PC-MRI. Because PC-MRI was collected before and after ACZ injection in each subject, we used separate images to calculate PC-PET quantitative CBF maps for pre- and post-ACZ.

Stenosis Grade of MM Patients and ROIs

The severity of stenosis of major cerebral arteries of MM was graded as normal, mild/moderate, or severe/occluded separately by two experienced clinicians (G.Z. and Y.I.), based on the MRA images (Fig. 2a), followed by a consensus session. Mild/moderate and severe/occluded groups were distinguished based on whether the distal arterial segments of the stenosis were depicted or not. In the case of ICA stenosis, this was regarded as stenosis of both the ipsilateral anterior and middle cerebral arteries (MCA). The presence of a fetal origin of the posterior cerebral artery (PCA) and hypoplasia of the anterior cerebral artery (ACA) were distinguished from stenosis.

After all PC-PET CBF images were normalized to the Montreal Neurological Institute (MNI) brain template, 20 standardized ROIs on brain cortex, corresponding roughly to the Alberta Stroke Program Early CT Score (ASPECTS) levels,[17] were overlaid onto the brain template in two axial planes, at the level of the basal ganglia and just above the superior aspect of the lateral ventricle (Fig. 2b). The use of ASPECTS regions allows for the measured regional CBF values to have direct relevance to vascular territories of the major cerebral arteries. Any ROIs with prior infarctions based on T_1-weighted imaging were excluded. All other ROIs were classified into three groups (normal, mild/moderate, severe/occluded) depending on the grade of the supplying cerebral artery stenosis in MM. We also evaluated healthy control subject findings and classified them as "HC" for comparison purposes.

Statistical Analysis

COMPARISON OF CBF WITH LITERATURE VALUE IN HCS.—To demonstrate the reliability of our method, PC-PET CBF values from whole brain (WB), gray matter (GM),

and white matter (WM) and the values of CVR in HC were compared with those reported in the literature since 2000. The literature describing the mean CBF of WB, GM, or WM in healthy adults measured using $H_2{}^{15}O$-PET with arterial blood sampling for AIF were included. Studies from the same institution where subjects overlapped and studies including fewer than 10 healthy subjects were excluded. In total, 13 articles were included.[9,14,18–28]

All images were analyzed in the MNI brain template space such that mean CBF measured at baseline and post-ACZ injection corresponded with the same GM and WM masks. FSL's standard WB mask template (MNI152_T1_2mm_brain_mask. nii) was adopted as the WB mask. The GM and the WM masks were obtained by binarizing the GM and the WM tissue priors provided by FSL (avg152T1_gray.nii and avg152T1_white.nii) using a threshold of 70 for the GM mask and 230 for the WM mask. The cerebellum was removed from both masks. The relationship between WB-CBF and the subject's hematocrit, between GM-CBF and the subject's age, and between GM/WM CBF ratio and the subject's age were evaluated by linear regression analysis.

COMPARISON OF PC-PET CBF AND CVR IN HCS AND MM DISEASE.—Regional values of CBF and CVR, defined as percent CBF change between baseline and post-ACZ scans, were calculated for HCs and MM patients. Each subject contributed 20 total regional values of CBF and CVR corresponding to three supplying cerebral arteries (ACA, MCA, and PCA) of the left and right side of the brain.

Linear, mixed effects models were created to evaluate CBF as an outcome measure. The first model evaluated whether CBF in HCs and normal regions in MM patients were different and fixed effects include the vessel territory (ACA, MCA, or PCA) and hemisphere (right or left). The second model evaluated whether CBF was related to stenosis grade in MM patients, and also fixed effects included the vessel territory and hemisphere. Similar, independent models were created to evaluate CVR as an outcome measure. All models considered the subjects as a random effect.

MEASUREMENTS WITH PHASE-CONTRAST MRI.—The measurements with PC-MRI were compared between baseline and post-ACZ injection scans, and between subgroup of HCs and MMs. Statistical analysis was performed using the Wilcoxon signed-rank test and the Wilcoxon rank sum test, respectively. Bonferroni correction was applied to account for multiple testing.

All data are presented as mean ± standard deviation (unless otherwise noted). The statistical analyses were performed with Stata v. 15.1 software (StataCorp, College Station, TX) except for analysis of the total blood inflow by phase-contrast MRI using JMP v. 14.1.0 software (SAS, Cary, NC). Probability values <0.05 were considered significant.

Results

PC-PET CBF in the HC Group

In healthy volunteers, baseline PC-PET CBF in the WB, all GM, and all WM regions are shown in Fig. 3: WB: 41.9 ± 6.6 ml/100 g/min, GM: 50.4 ± 7.3 ml/100 g/min, WM: 22.5 ±

3.1 ml/100 g/min. After ACZ administration, CBF increased significantly (WB: 65.4 ± 11.4ml/100 g/min, GM: 79.0 ± 13.4 ml/100 g/min, and WM: 34.9 ± 7.9 ml/100 g/min). The mean values of CVR for WB, GM, and WM were 57.2 ± 23.9%, 57.7 ± 23.6%, and 55.8 ± 30.6%, respectively. The mean value of GM/WM CBF ratio was 2.3 ± 0.3 for both the baseline and post-ACZ scans.

Baseline CBF values from PC-PET in this study were comparable to previous $H_2{}^{15}O$-PET CBF studies: WB 43.2 ± 6.6 (range: 28.2–59.0) ml/100 g/min,[9,14,18–20,24,25,27,28] GM 52.0 ± 8.8 (range: 34.5–67.0) ml/100 g/min,[9,14,18,21–23,25,26] WM 22.2 ± 3.6 (range: 17.4–33.0) ml/100 g/min,[9,14,18,22,23,25] respectively, and GM/WM CBF ratio of 2.3 ± 0.7 (range: 1.4–3.2).[9,14,18,22,23,25]

WB baseline CBF values from PC-PET in HC showed significant negative correlation with hematocrit ($r = -0.65$, $P = 0.022$) (Fig. 4a). We also found a significant negative correlation between PC-PET WB-CBF and age ($r = -0.60$, $P = 0.037$), and between GM/WM CBF ratio and age ($r = -0.80$, $P = 0.0017$) (Fig. 4B,C).

Comparison of PC-PET CBF and CVR Between Stenosis Grades

The consensus ratings of MRA stenosis grade in patients are presented in Table 2. The kappa value for interobserver agreement was 0.68. After consensus, 50% of cerebral arteries were determined to be normal, 31% mildly/moderately stenosed, and 19% severely stenosed or occluded. As expected for MM disease, there was a low frequency of posterior involvement; only 1/26 PCAs was abnormal and this vessel had mild/moderate stenosis. Only 2/52 ROIs perfused by the PCA and 2/156 ROIs perfused by the MCA were excluded due to chronic infarction. Figure 5 shows representative cases of MRA, baseline and post-ACZ CBF, change in CBF (ΔCBF), and CVR (% change) in patients with each stenosis grade.

Regression analysis for ASPECTS ROIs showed there was no significant difference in baseline PC-PET CBF values between HCs and regions supplied by normal vessels in MM patients (50.7 ± 7.7 ml/100 g/min vs. 47.3 ± 8.6 ml/100 g/min, $P = 0.132$). Similarly, CVR in normal regions of MM patients did not differ from that in HCs (57.9 ± 15.6% vs. 57.3 ± 23.1%, $P = 0.932$) (Fig. 6a,b).

In MM patients, compared with normal areas, ASPECTS regions with both mild/moderate and severe/occluded arteries did not show significantly different baseline CBF: mild/moderate 43.5 ± 7.7 ml/100 g/min, $P = 0.835$; severe/occluded 40.1 ± 5.4 ml/100 g/min, $P = 0.374$ (Fig. 6a). However, CVR was significantly decreased in areas with mild/moderate stenosis (47.3 ± 16.9%, $P = 0.011$) and in severe/occluded areas (40.2 ± 15.6%, $P = 0.016$) compared with normal regions in MM patients (Fig. 6b). Table 3 shows the values of baseline CBF, post-ACZ CBF, and CVR in regions supplied by the different arterial stenosis grades for all subjects.

Measurements With Phase-Contrast MRI

PC-MRI measured blood flow data are presented in Table 4. Mean flow velocity significantly increased in the ICAs and VAs after ACZ injection in both groups. The blood flow in ICAs, VAs, and the total blood inflow significantly increased after ACZ injection in

HCs, and the blood flow in VAs and the total blood inflow significantly increased in MM disease patients.

The cross-sectional area of the ICAs on the post-ACZ scan in HCs was significantly larger than in MM patients. The blood flow in ICAs in HCs was also larger than in MM patients on both baseline and post-ACZ scans. The VAs in MM patients, however, had significantly larger flow velocity on both baseline and post-ACZ scans than in HCs. The blood flow of VAs in MM patients was also correspondingly larger than in HCs on both baseline and post-ACZ scans.

Discussion

The aim of this study was to demonstrate that the new CBF measurement method, PC-PET, gives absolute CBF values in the physiological range for normal controls, and detects regional cerebral perfusion impairment in cerebrovascular disease. This study had two major findings. First, CBF measured by PC-PET agreed with the literature values in healthy subjects and behaved as expected with hematocrit and age. Second, the absolute value maps of CVR derived from PC-PET showed correlation with stenosis grade in the patients with MM disease.

PC-PET is an absolute quantification method for $H_2{}^{15}O$PET CBF that uses PC-MRI data as a scale instead of using an AIF with arterial blood sampling. This method has two major advantages: 1) it is noninvasive and 2) it is not affected by tracer delays and dispersions.[5] In this study we used a PET/MRI scanner to simultaneously measure blood flow distribution by $H_2{}^{15}O$-PET and total blood inflow by PC-MRI. The simultaneous PET/MRI scanner enables PC-PET since it allows the evaluation of the same state of brain hemodynamics on two modalities and excludes physiological variability between scanning sessions.

In a recent review of PET and arterial spin labeling (ASL)-MRI CBF comparison studies, it was demonstrated that the strength of correlation between two modalities is heavily influenced by the time interval between the examinations.[29] This observation suggests that spacing the $H_2{}^{15}O$-PET and PC-MRI acquisitions closely in time is important for the PC-PET method, and that simultaneous measurement is ideal.

PC-MRI measurements such as blood flow rate, flow velocity, vessel diameter, and total blood inflow of ICA and VA in our study were comparable to previous reports in healthy controls.[10,15] Furthermore, PC-PET showed similar CBF values in the WB, GM, and WM to the average of the ^{15}O-PET CBF values with arterial sampling in previous literature.[9,14,18–28] In those reports, however, average CBF differed by a factor of two between studies, suggesting that CBF derived from ^{15}O-PET widely differs depending on subjects' characteristics including age and gender, institutions, ROI selection, analysis techniques, scanners, and other factors. We note that our healthy volunteers were age- and gender-matched to the MM patient cohort and thus includes a higher proportion of females compared with many previous studies.

To evaluate the reliability of PC-PET, we also related PC-PET in HCs to hematocrit and age. Prior research has confirmed that hematocrit influences the blood's viscosity and arterial

oxygen content, and the average CBF is negatively correlated with hematocrit.[30] In this study, a significant negative correlation was observed between WB PC-PET CBF and hematocrit. CBF in WB and GM has also been shown to negatively correlate with age, with a rate of decrease of 0.38–0.76% per year.[31] In this study, the rate of decrease in WB CBF with age was 0.46% per year. Moreover, the GM/WM ratio of CBF is reported to have an even stronger correlation with age.[32] In this study as well, subjects' age showed a stronger correlation with GM/WM ratio than WB CBF. These findings support the validity of the WB measurements (from PC-MRI) and the GM/WM distribution of CBF (from the PET scan) that comprise our PC-PET methodology.

In this work, we evaluated CVR in MM patients by the ACZ test and imaging with PC-PET. In normal vascular regions of MM patients, CVR was found to be similar to HCs. With the progression of stenosis, however, CVR decreased significantly. Compared with the normal vascular regions, CVR was 18% lower in the regions corresponding to mild or moderately stenosed arteries; and 31% lower in regions corresponding to severe or occluded arteries. The results of the current study are consistent with prior reports that the extent of vascular steno-occlusion in MM disease negatively correlates with CVR derived from MRI.[33,34] Since CVR is calculated from the subtraction of two CBF measurements, several potential sources of measurement error exist. To create an accurate CVR map, reproducibility of absolute CBF values and accurate coregistration of CBF images is indispensable. The inverse correlation between CVR and corresponding arterial stenosis grade supports the reliability of PC-PET, and it also shows that PCPET can detect abnormal perfusion areas in chronic ischemic cerebrovascular patients.

Unlike CVR, we did not observe a correlation between the severity of stenosis and baseline CBF within the corresponding regions. Some previous studies have found a relationship between stenosis classification on conventional angiography and baseline cerebral prefusion, [35] but others showed that baseline CBF did not relate to angiographic findings of the major cerebral arteries.[34] The reason for these divergent findings is that regional CBF is strongly influenced by the collateral circulation via MM vessels and leptomeningeal anastomosis, and not only by the lesion of the major cerebral arteries.[36] In consequence, CVR is likely more sensitive to pathophysiology and severity in MM disease than baseline CBF.

Using ACZ in healthy people with $H_2{}^{15}O$-PET or single photon emission tomography (SPECT), WB CVR values in HCs have been reported to be 30–40%.[37] The value of CVR in HC in the present study was 57%, which is in the expected physiological range but higher than many previously reported values. Previous methodology may have limitations. For example, SPECT and even PET have been shown to underestimate CBF because of limited permeability of the tracer in high perfusion conditions, which may lead to underestimation of true CVR in healthy controls.[38] However, within the physiological range of CBF, the effects of limited water extraction are minor for $H_2{}^{15}O$-PET; less than 10% underestimation for true CBF values as high as 60 ml/100g/min, so O-15-water PET can still be regarded as the gold standard for CBF measurement, especially in baseline states.

There are several limitations in this research. First, this method has not been compared with a reference standard such as PET with arterial blood sampling. In the original article by Ssali

et al using a porcine model, a good correlation was reported between WB CBF measured by $H_2{}^{15}O$-PET and PC-MRI.[11] On the other hand, Vestergaard et al found in healthy males that PC-MRI significantly overestimates WB CBF compared with $H_2{}^{15}O$-PET (with blood sampling) by up to 63%.[10] Reliability of PC-PET essentially depends on the global CBF from PC-MRI. Our global CBF values (42 ml/100g/mi) agree better with average literature values and are likely more accurate than those in Vestergaard et al's study due to improved spatial resolution[39] and use of cardiac triggering[8] in our PC-MRI acquisition. More recently, Puig et al compared fully quantitative $H_2{}^{15}O$-PET with PC-MRI at baseline and after ACZ injection in healthy volunteers on a hybrid PET/MRI system. Although the CVR was comparable with moderate correlation, the absolute value of CBF measured by PC-MRI was again higher compared with PET.[40] Furthermore, no studies have validated the accuracy of PCMRI against PET in steno-occlusive disease. Our observation that PC-PET measured CVR corresponded to the severity of disease is a new finding and is a foundation for future PCMRI and PET validation studies in patients with steno-occlusive disease.

Second, we assumed that summed counts in $H_2{}^{15}O$PET static scans reflect the distribution of blood flow. In Herscovitch et al's original article about the autoradiographic method, the number of local tissue counts was demonstrated in theory to relate almost linearly to flow.[4] We have not evaluated, however, the 2-minute timeframe for static PET with other acquisition intervals. Longer data acquisition intervals in static PET provide more total coincidence counts and therefore higher statistical accuracy. However, late timepoints in PET become less dependent on flow and more dependent on the blood–tissue partition coefficient.[41] We adopted 2 minutes as the acquisition interval similar to previous reports,[32] but determining the optimal interval requires further analysis.

Third, the measurement of the blood flow in four feeding arteries on a single plane by PC-MRI has limitations. A previous report showed no significant blood flow difference in PC-MRI measurements if the imaging slice angulation was within 10 from the ideal orientation (perpendicular to the vessel segment). An angulation of 20 between the imaging plane and artery, however, showed a significant overestimation of ICA and VA blood flow by 9.3% and 13%, respectively.[39] The average deviation of the slice from ideal angulation in our study is less than 10; therefore, we considered the error of blood flow in our method to be acceptable. In total, 7 out of 100 arteries (7%) measured showed an angle of 15 or more, which may overestimate the blood flow by around 10%. In addition, the Venc for PC-MRI acquisitions should be selected to accommodate the maximal flow velocity, including after ACZ. While our selected Venc = 100 cm/s was appropriate for our cohorts and did not lead to phase aliasing, the Venc may need to be increased for patients with other pathologies such as sickle cell anemia.

Finally, spontaneous collateral flow from the external carotid arteries in MM patients can lead to CBF underestimation with the PC-PET method because these arteries are not included in the PC-MRI measurement. If it is assumed that the collateral flow rate from the external carotid artery is close to the average graft flow rate for the superficial temporal artery / middle cerebral artery in the setting of bypass surgery for MM patients, reported to be 21 ml/min,[42] this causes ~8% underestimation of total blood inflow for MM patients in PCPET at baseline. Note that we do not expect this error to occur in the HC cohort. And, for

MM patients, prominent extradural vessels can be identified and their flow measured with PC-MRI to include in the global CBF measurement.

In conclusion, we found that PC-PET provides quantitative CBF and CVR measurement comparable with $H_2{}^{15}$OPET with arterial blood sampling in humans. This new method measures absolute CBF from $H_2{}^{15}$O-PET with quantitative scaling using WB CBF by PC-MRI instead of arterial blood sampling. PC-PET is facilitated by simultaneous cross-modality measurements using hybrid PET-MRI. We observed meaningful correlations between cerebrovascular stenosis degree and PC-PET CVR values in patients with MM disease. Moreover, the achieved PC-PET CBF values were highly consistent with literature values in HCs. Based on the present study, PCPET can be advocated when arterial cannulation is not possible or not acceptable. However, whether PC-PET can be used as a reliable alternative to fully quantitative $H_2{}^{15}$O-PET needs further evaluation of both methods in the same cohort, particularly for clinical use.

Acknowledgments

The authors thank Omar Rutledge and Andrea Otte for support in patient recruitment and Tie Liang for statistical analysis. The authors also acknowledge the support of the technologists and clinical fellows at Stanford Healthcare.

References

1. Derdeyn CP, Videen TO, Yundt KD, et al. Variability of cerebral blood volume and oxygen extraction: Stages of cerebral haemodynamic impairment revisited. Brain 2002;125:595–607. [PubMed: 11872616]
2. Suzuki J, Kodama N. Moyamoya disease—A review. Stroke 1983;14: 104–109. [PubMed: 6823678]
3. Gupta A, Chazen JL, Hartman M, et al. Cerebrovascular reserve and stroke risk in patients with carotid stenosis or occlusion: A systematic review and meta-analysis. Stroke J Cereb Circ 2012;43: 2884–2891.
4. Herscovitch P, Markham J, Raichle ME. Brain blood flow measured with intravenous H 2 15 O. I. Theory and error analysis. J Cereb Blood Flow Metab 1983;24:782–789.
5. Iida H, Kanno I, Miura S, Murakami M, Takahashi K, Uemura K. Error analysis of a quantitative cerebral blood flow measurement using H 2 15 O autoradiography and positron emission tomography, with respect to the dispersion of the input function. J Cereb Blood Flow Metab 1986; 6:536–545. [PubMed: 3489723]
6. Koopman T, Yaqub M, Heijtel DF, et al. Semi-quantitative cerebral blood flow parameters derived from non-invasive [15 O]H 2 O PET studies. J Cereb Blood Flow Metab 2017:0271678X1773065.
7. Khalighi MM, Deller TW, Fan AP, et al. Image-derived input function estimation on a TOF-enabled PET/MR for cerebral blood flow mapping. J Cereb Blood Flow Metab 2018;38:126–135. [PubMed: 28155582]
8. Spilt A, Box FMA, Geest RJ van der, et al. Reproducibility of total cerebral blood flow measurements using phase contrast magnetic resonance imaging. J Magn Reson Imaging 2002;16:1–5. [PubMed: 12112496]
9. Henriksen OM, Larsson HBW, Hansen AE, Grüner JM, Law I, Rostrup E. Estimation of intersubject variability of cerebral blood flow measurements using MRI and positron emission tomography. J Magn Reson Imaging 2012;35:1290–1299. [PubMed: 22246715]
10. Vestergaard MB, Lindberg U, Aachmann-Andersen NJ, et al. Comparison of global cerebral blood flow measured by phase-contrast mapping MRI with 15O-H2O positron emission tomography. J Magn Reson Imaging 2017;45:692–699. [PubMed: 27619317]
11. Ssali T, Anazodo UC, Thiessen JD, Prato FS, Lawrence KS. A noninvasive method for quantifying cerebral blood flow by hybrid PET/MR. J Nucl Med 2018 jnumed.117.203414.

12. Aslan S, Xu F, Wang PL, et al. Estimation of labeling efficiency in pseudocontinuous arterial spin labeling. Magn Reson Med 2010;63: 765–771. [PubMed: 20187183]
13. Wu W-C, St Lawrence KS, Licht DJ, Wang DJJ. Quantification issues in arterial spin labeling perfusion magnetic resonance imaging. Top Magn Reson Imaging 2010;21:65. [PubMed: 21613872]
14. Zhang K, Herzog H, Mauler J, et al. Comparison of cerebral blood flow acquired by simultaneous [15 O]water positron emission tomography and arterial spin labeling magnetic resonance imaging. J Cereb Blood Flow Metab 2014;34:1373–1380. [PubMed: 24849665]
15. Neff KW, Horn P, Schmiedek P, Düber C, Dinter DJ. 2D cine phase-contrast MRI for volume flow evaluation of the brain-supplying circulation in Moyamoya disease. Am J Roentgenol 2006;187: W107–W115. [PubMed: 16794123]
16. Sekine T, Buck A, Delso G, et al. Evaluation of atlas-based attenuation correction for integrated PET/MR in human brain: Application of a head atlas and comparison to true CT-based attenuation correction. J Nucl Med 2016;57:215–220. [PubMed: 26493207]
17. Kim JJ, Fischbein NJ, Lu Y, Pham D, Dillon WP. Regional angiographic grading system for collateral flow: Correlation with cerebral infarction in patients with middle cerebral artery occlusion. Stroke 2004;35: 1340–1344. [PubMed: 15087564]
18. Ye FQ, Berman KF, Ellmore T, et al. H 2 15 O PET validation of steady-state arterial spin tagging cerebral blood flow measurements in humans. Magn Reson Med 2000;44:450–456. [PubMed: 10975898]
19. Okazawa H, Vafaee M. Effect of vascular radioactivity on regional values of cerebral blood flow: Evaluation of methods for H 2 15 O PET to distinguish cerebral perfusion from blood volume. J Nucl Med 2001; 42:1032–1039. [PubMed: 11438623]
20. Moore DF, Altarescu G, Herscovitch P, Schiffmann R. Enzyme replacement reverses abnormal cerebrovascular responses in Fabry disease. BMC Neurol 2002;2:4. [PubMed: 12079501]
21. Hattori N, Huang S-C, Wu H-M, et al. Acute changes in regional cerebral 18f-fdg kinetics in patients with traumatic brain injury. J Nucl Med 2004;45:775–783. [PubMed: 15136626]
22. Rostrup E, Knudsen GM, Law I, Holm S, Larsson HBW, Paulson OB. The relationship between cerebral blood flow and volume in humans. NeuroImage 2005;24:1–11. [PubMed: 15588591]
23. Grandin CB, Bol A, Smith AM, Michel C, Cosnard G. Absolute CBF and CBV measurements by MRI bolus tracking before and after acetazolamide challenge: Repeatabilily and comparison with PET in humans. NeuroImage 2005;26:525–535. [PubMed: 15907309]
24. Coles JP, Fryer TD, Bradley PG, et al. Intersubject variability and reproducibility of 15O PET studies. J Cereb Blood Flow Metab 2006;26: 48–57. [PubMed: 15988475]
25. Golen LW van Kuijer JPA, Huisman MC, et al. Quantification of cerebral blood flow in healthy volunteers and type 1 diabetic patients: Comparison of MRI arterial spin labeling and [15 O]H2O positron emission tomography (PET). J Magn Reson Imaging 2014;40:1300–1309. [PubMed: 24214919]
26. Heijtel DFR, Mutsaerts HJMM, Bakker E, et al. Accuracy and precision of pseudo-continuous arterial spin labeling perfusion during baseline and hypercapnia: A head-to-head comparison with 15O H 2 O positron emission tomography. NeuroImage 2014;92:182–192. [PubMed: 24531046]
27. Hiura M, Nariai T, Ishii K, et al. Changes in cerebral blood flow during steady-state cycling exercise: A study using oxygen-15-labeled water with PET. J Cereb Blood Flow Metab 2014;34:389–396. [PubMed: 24301294]
28. Okazawa H, Higashino Y, Tsujikawa T, et al. Noninvasive method for measurement of cerebral blood flow using O-15 water PET/MRI with ASL correlation. Eur J Radiol 2018;105:102–109. [PubMed: 30017265]
29. Fan AP, Jahanian H, Holdsworth SJ, Zaharchuk G. Comparison of cerebral blood flow measurement with [15 O]-water positron emission tomography and arterial spin labeling magnetic resonance imaging: A systematic review. J Cereb Blood Flow Metab 2016;36:842–861. [PubMed: 26945019]
30. Kusunoki M, Kimura K, Nakamura M, Isaka Y, Yoneda S, Abe H. Effects of hematocrit variations on cerebral blood flow and oxygen transport in ischemic cerebrovascular disease. J Cereb Blood Flow Metab 1981;1: 413–417. [PubMed: 7328151]

31. Chen JJ, Rosas HD, Salat DH. Age-associated reductions in cerebral blood flow are independent from regional atrophy. NeuroImage 2011; 55:468–478. [PubMed: 21167947]
32. Xu G, Rowley HA, Wu G, et al. Reliability and precision of pseudocontinuous arterial spin labeling perfusion MRI on 3.0 T and comparison with 15O-water PET in elderly subjects at risk for Alzheimer's disease. NMR Biomed 2010;23:286–293. [PubMed: 19953503]
33. Donahue MJ, Ayad M, Moore R, et al. Relationships between hypercarbic reactivity, cerebral blood flow, and arterial circulation times in patients with moyamoya disease. J Magn Reson Imaging 2013;38: 1129–1139. [PubMed: 23440909]
34. Federau C, Christensen S, Zun Z, et al. Cerebral blood flow, transit time, and apparent diffusion coefficient in moyamoya disease before and after acetazolamide. Neuroradiology 2017;59:5–12. [PubMed: 27913820]
35. Togao O, Mihara F, Yoshiura T, et al. Cerebral hemodynamics in Moyamoya disease: Correlation between perfusion-weighted MR imaging and cerebral angiography. Am J Neuroradiol 2006;27:391–397. [PubMed: 16484417]
36. Zaharchuk G, Do HM, Marks MP, Rosenberg J, Moseley ME, Steinberg GK. Arterial spin-labeling MRI can identify the presence and intensity of collateral perfusion in patients with Moyamoya disease. Stroke 2011;42:2485–2491. [PubMed: 21799169]
37. Boles Ponto LL, Schultz SK, Leonard Watkins G, Hichwa RD. Technical issues in the determination of cerebrovascular reserve in elderly subjects using 15O-water PET imaging. NeuroImage 2004;21: 201–210. [PubMed: 14741657]
38. Iida H, Akutsu T, Endo K, et al. A multicenter validation of regional cerebral blood flow quantitation using [123 I]Iodoamphetamine and single photon emission computed tomography. J Cereb Blood Flow Metab 1996;16:781–793. [PubMed: 8784223]
39. Peng S-L, Su P, Wang F-N, et al. Optimization of phase-contrast MRI for the quantification of whole-brain cerebral blood flow. J Magn Reson Imaging 2015;42:1126–1133. [PubMed: 25676350]
40. Puig O, Vestergaard MB, Lindberg U, et al. Phase contrast mapping MRI measurements of global cerebral blood flow across different perfusion states —A direct comparison with ^{15}O-H$_2$O positron emission tomography using a hybrid PET/MR system. J Cereb Blood Flow Metab 2018:0271678X1879876.
41. Koeppe RA, Hutchins GD, Rothley JM, Hichwa RD. Examination of assumptions for local cerebral blood flow studies in PET. J Nucl Med 1987;28:1695–1703. [PubMed: 3499491]
42. Lee M, Guzman R, Bell-Stephens T, Steinberg GK. Intraoperative blood flow analysis of direct revascularization procedures in patients with Moyamoya disease. J Cereb Blood Flow Metab 2011;31:262–274. [PubMed: 20588321]

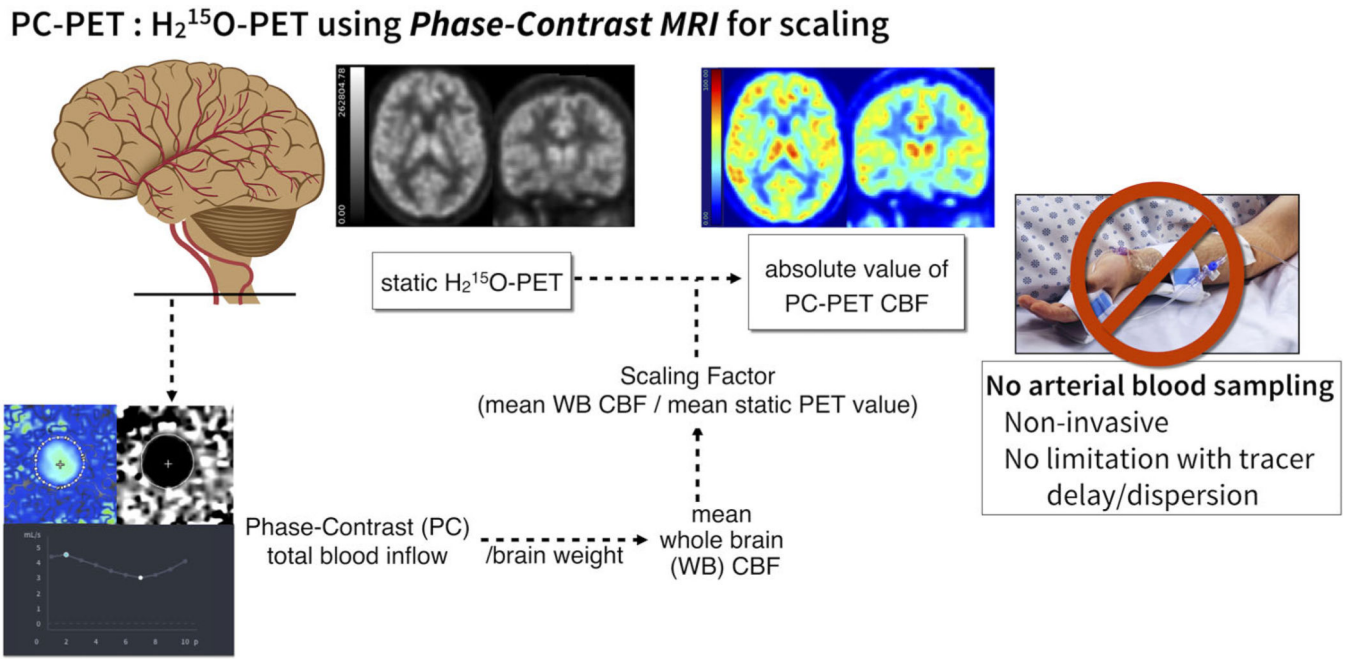

FIGURE 1:

Schematic flow chart of PC PET method. A scan-specific scaling factor is calculated to scale the static O-15 water PET counts (2 min), to be consistent with WB CBF determined from a simultaneous PC scan. The WB CBF is derived from PC total blood inflow is normalized with brain volume estimated from a segmented 3D T_1-weighted anatomical MR-scan. The static $H_2{}^{15}O$ PET volume is then scaled to the WB CBF value to achieve a quantitative map of CBF in absolute units.

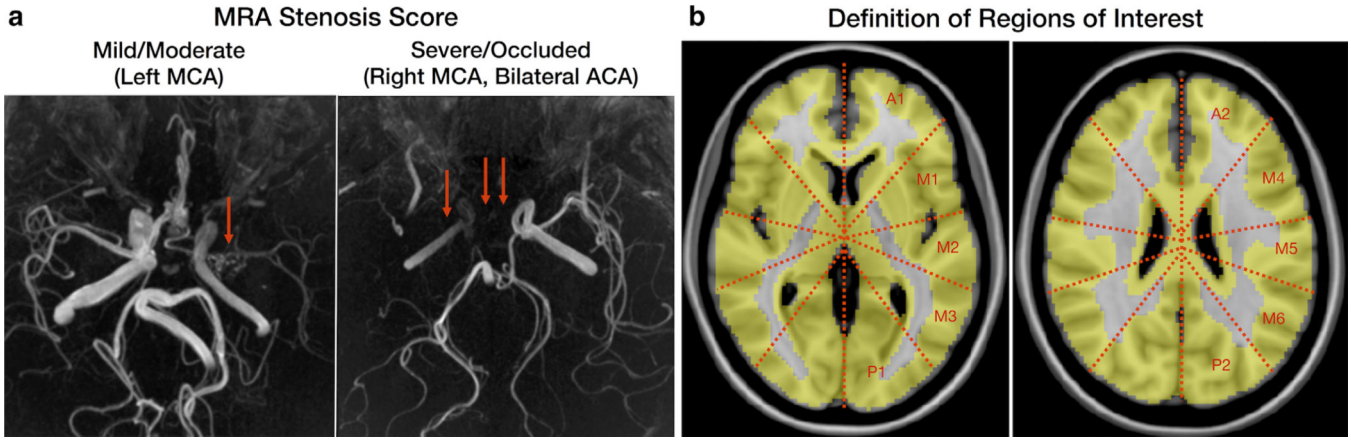

FIGURE 2:

a: Representative images of the MRA stenosis score. Cerebral arteries with stenotic lesions but visualized along their expected full length were graded as mild/moderate stenosis (left image). Cerebral arteries with stenotic lesions visualized only partly or only in their proximal segments were graded as severe/occluded (right image). **b:** Standardized ROIs in 10 perfusion territories (two anterior, six middle, and two posterior) per hemisphere, corresponding to two slice locations of the ASPECTS on the MNI template.

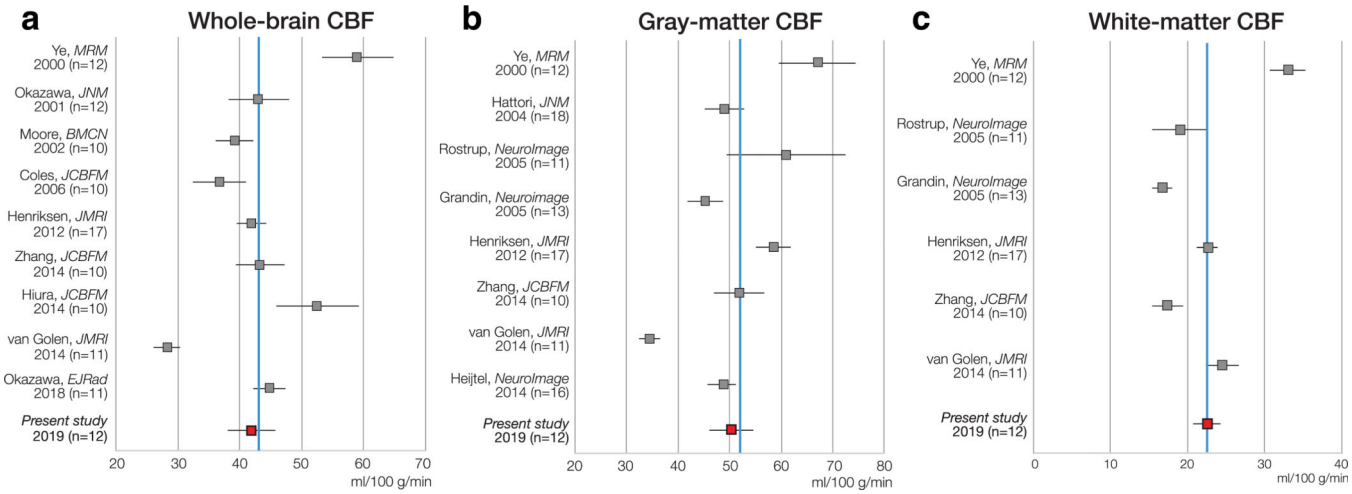

FIGURE 3:

PC-PET CBF in healthy controls compared with literature values derived from $H_2{}^{15}O$-PET across the WB (a), the GM (b), and WM (c). Error bars are estimated 95% confidence intervals that account for the standard deviation and the sample size of each study. The solid blue line represents the mean $H_2{}^{15}O$-PET CBF value across the studies. PC: phase-contrast, PET: positron emission tomography.

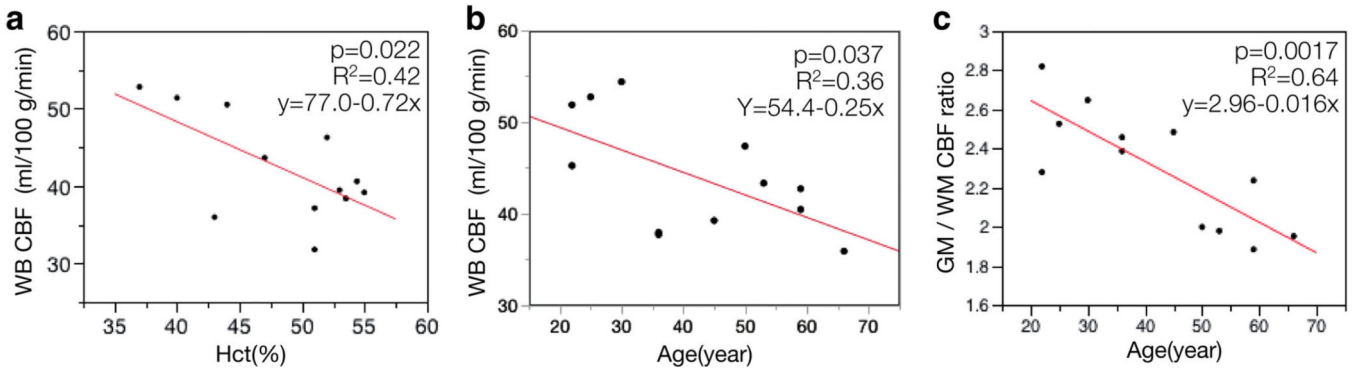

FIGURE 4:

a: Association between PC-PET CBF and hematocrit (Hct). **b:** Association between PC-PET CBF and age. **c:** Association between GM/WM CBF ratio and age. There were significant inverse correlations ($P < 0.05$) in each of the scatterplots (a–c). CBF: cerebral blood flow, PC: phase-contrast, PET: positron emission tomography, WB: whole brain, Hct: hematocrit, GM: gray matter, WM: white matter.

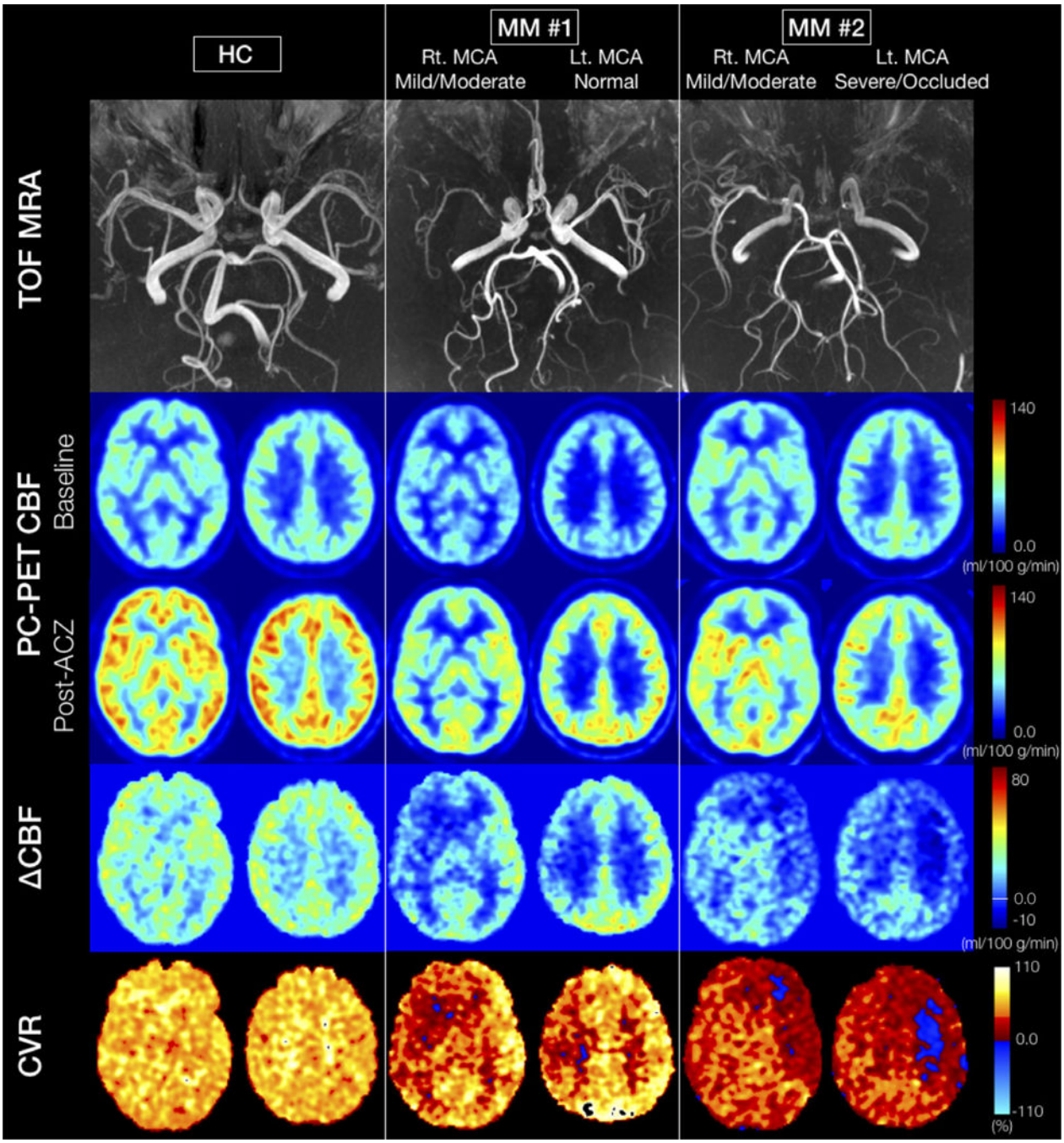

FIGURE 5:

Representative cases: (From the top row) TOF MR angiogram, two slices of PC-PET CBF at baseline and after ACZ administration, change in CBF (ΔCBF), and cerebrovascular reactivity (CVR, %) maps. The left column shows an HC case. A significant CBF increase is visible in all territories after ACZ. The ΔCBF in GM is larger than deep WM, while CVR is essentially constant in all regions for the HC. The middle and right columns show the patients with Moyamoya disease. Both cases present asymmetrical stenosis grades for each MCA with normal grades for the bilateral PCAs. Bilateral ACAs are graded as normal in

Patient #1 and as severe in Patient #2. The post-ACZ CBF is obviously asymmetrical, with less CBF increase on the hemisphere with more severe artery stenosis in both MM cases. In particular, in the left hemisphere of Patient #2, there are regions where the CVR is negative (blue area). HC: healthy control, TOF: time of flight, ACZ: acetazolamide, PC: phase-contrast, PET: positron emission tomography, CBF: cerebral blood flow, CVR: cerebrovascular reactivity, MCA: middle cerebral artery, PCA: posterior cerebral artery, ACA: anterior cerebral artery.

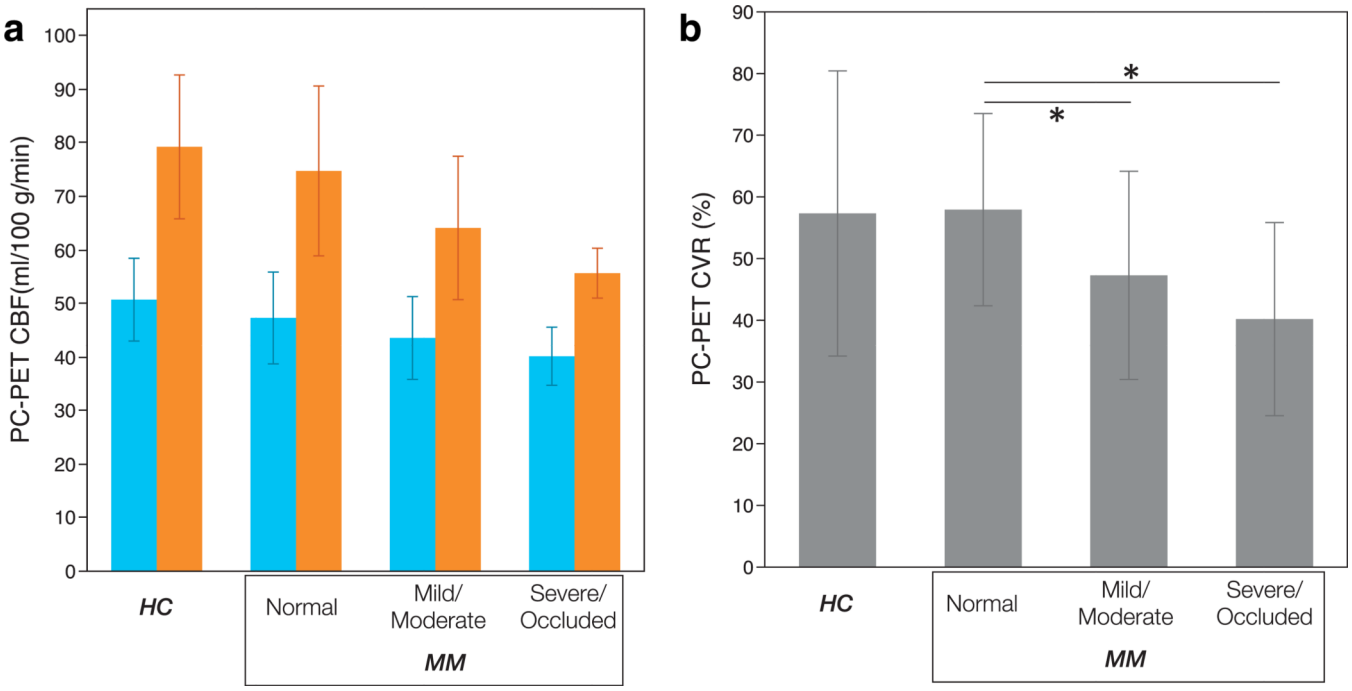

FIGURE 6:

PC-PET CBF (a) and CVR (b) was compared by MR angiogram stenosis grades (for MM patients) as well as for HC for ASPECTS cortical regions. No differences in baseline CBF were identified between grades of stenosis. However, regions in Moyamoya patients corresponding to mild/moderately stenosis and severe/occluded arteries showed lower CBF than in normal regions. Blue and orange bars in (a) show the CBF of baseline and post-ACZ scan, respectively. The error bars show standard deviation. Asterisks indicate significant difference at the $P < 0.05$ level. HC: healthy control, MM: patients with Moyamoya disease, PC: phase-contrast, PET: positron emission tomography, CBF: cerebral blood flow, CVR: cerebrovascular reactivity.

TABLE 1.

Subject Characteristics

	HC (*n* = 12)	MM (*n* = 13)	*P* value
Age (years)	41.9 ± 15.5	39.5 ± 15.4	0.67
Sex	9 Female	10 Female	0.91
Body weight (kg)	73.7 ± 16.6	77.8 ± 15.2	0.52
Baseline HR (beat/min)	63.2 ± 6.4	67.4 ± 12.0	0.29
Post-ACZ HR (beat/min)	67.2 ± 8.5	70.9 ± 11.1	0.36
Hematocrit (%)	47.3 ± 6.3	46.9 ± 7.4	0.90
Total brain volume (ml)	1446 ± 140	1405 ± 173	0.49
Total brain weight (g)	1591 ± 154	1540 ± 190	0.49

HR: heart rate, ACZ: acetazolamide, HC: healthy control, MM: Moyamoya disease.

J Magn Reson Imaging. Author manuscript; available in PMC 2020 May 11.

TABLE 2.

Results of MRA Stenosis Score

	Left			Right			
MRA score	**ACA**	**MCA**	**PCA**	**ACA**	**MCA**	**PCA**	**Total**
Normal	3 (23%)	4 (31%)	13 (100%)	4 (31%)	3 (23%)	12 (92%)	39 (50%)
Mild/moderate	5 (38%)	4 (31%)	0 (0%)	6 (46%)	8 (62%)	1 (8%)	24 (31%)
Severe/occluded	5 (38%)	5 (38%)	0 (0%)	3 (23%)	2 (15%)	0 (0%)	15 (19%)

The denominator of each percentage is the number of subjects (13), except in the “Total” column, where it is the total number of cerebral arteries (78). ACA: anterior cerebral artery, MCA: middle cerebral artery, PCA: posterior cerebral artery.

TABLE 3.

PC-PET CBF and CVR in Each Cerebral Artery Perfusion Territory (ASPECTS Regions)

		Baseline CBF (ml/100 g/min)			Post-ACZ CBF (ml/100 g/min) (CVR(%))		
		ACA	**MCA**	**PCA**	**ACA**	**MCA**	**PCA**
HC		48.8 ± 7.7	51.5 ± 8.1	50.2 ± 6.4	75.8 ± 12.2	80.6 ± 13.7	78.7 ± 13.3
					(56.6 ± 23.0)	(57.5 ± 23.1)	(57.5 ± 23.6)
MM	Normal	47.6 ± 9.0	49.3 ± 8.9	45.4 ± 7.9	73.8 ± 15.7	79.7 ± 18.1	70.7 ± 12.6
					(54.6 ± 14.6)	(61.0 ± 17.8)	(56.4 ± 13.6)
	Mild/moderate	40.7 ± 6.4	44.5 ± 8.0	41.3 ± 1.1	58.4 ± 12.7	65.7 ± 13.4	68.2 ± 4.6
					(43.6 ± 18.3)	(47.9 ± 16.4)	(65.0 ± 6.7)
	Severe/occluded	38.0 ± 4.8	40.9 ± 5.5	—	54.3 ± 6.2	56.1 ± 3.9	—
					(43.8 ± 17.5)	(38.9 ± 15.0)	
	Total	42.2 ± 8.1	45.0 ± 8.4	45.1 ± 7.9	62.2 ± 15.1	67.3 ± 16.2	70.7 ± 12.6
					(47.1 ± 18.1)	(49.4 ± 18.8)	(57.2 ± 13.5)

TABLE 4.

Summary of Phase-Contrast MRI Measurements

			Flow velocity (cm/s)	Area (mm^2)	Blood flow (ml/min)	Total blood inflow (ml/min)	Imaging angle deviation from ideal plane (deg)
HC	Baseline	ICA	37.2 ± 9.0	19.0 ± 5.3	255 ± 56	668 ± 131	8.4 ± 6.2 (0.2 − 22.7)
		VA	22.9 ± 6.0	11.1 ± 8.4	78 ± 36		8.2 ± 4.3 (1.2 − 17.3)
	Post-ACZ	ICA	48.1 ± 10.4 [a]<0.001	23.1 ± 6.1 [a]<0.001	395 ± 78 [a]<0.001	1039 ± 201 [a]<0.001	
		VA	29.7 ± 5.8 [a]<0.001	11.9 ± 4.5	125 ± 55 [a]< 0.001		
MM	Baseline	ICA	32.3 ± 10.6	15.4 ± 7.9	146 ± 96 [b]<0.001	530 ± 121	5.6 ± 4.0 (0.2 − 15.6)
		VA	31.0 ± 8.6 [c]<0.001	11.1 ± 3.9	119 ± 57 [c]0.0045		6.4 ± 4.7 (1.1 − 19.2)
	Post-ACZ	ICA	39.3 ± 14.0 [a]<0.001	16.2 ± 7.6 [b]0.0026	220 ± 156 [b]<0.001	805 ± 232 [a]0.0049	
		VA	40.8 ± 8.6 [a]<0.001 [c]<0.001	13.2 ± 3.8 [a]<0.001	182 ± 77 [a]<0.001 [c]0.0053		

[a]Significant difference from baseline was shown.

[b]Significant difference from healthy control was shown (HC>MM).

[c]Significant difference from healthy control was shown (HC<MM), ACZ: acetazolamide, ICA: internal carotid artery, VA: vertebral artery.

J Magn Reson Imaging. Author manuscript; available in PMC 2020 May 11.